A comparison of registration methods for SLAM with the M8 Quanergy LiDAR

Marina Aguilar-Moreno, Manuel Graña

Computational Intelligence Group, University of the Basque Country (UPV/EHU), San Sebastian, Spain

Abstract. LiDAR based SLAM is becoming affordable by new sensors such as the M8 Quanergy LiDAR, but there is still little work reporting on the accuracy attained with them. In this paper we report on the comparison of three registration methods applied to the estimation of the path followed by the LiDAR sensor and the registration of the overall cloud of points, namely the iterated closest points (ICP), Coherent Point Drift (CPD), and Normal Distributions Transform (NDT) registration methods. In our experiment, we found that the NDT method provides the most robust performance.

Keywords: Point Cloud Registration · LiDAR · SLAM.

1 Introduction

The simultaneous localization and mapping (SLAM) aims to estimate a reconstruction of the environment along with the path traversed by the sensor has become an integral part of the robotic operating system (ROS) [13,14]. One of the most widely used kinds of sensors used for SLAM are laser based depth measurement sensors, or light detection and ranging (LiDAR) sensors, which have been used for scanning and reconstruction of indoor and outdoor environments [3], even in underground mining vehicles [12]. Fusion of LiDAR with GPS allows for large scale navigation [4] of autonomous systems.

New affordable LiDAR sensors, such as the M8 from Quanergy that we are testing in this paper, allow for further popularization of LiDAR based SLAM applications. Due to its specific innovative characteristics, the M8 sensor still needs extensive testing by the community in order to assume its integration in the newly developed systems [9]. The work reported in this paper is intended partly to provide such empirical confirmation of the M8 sensor quality. We have not carried out any precise calibration process of the sensor [5,6]. Instead, we are assessing the sensor through the comparison of three standard point cloud registration methods over experimental data gathered inhouse.

This paper is structured as follow: A brief presentation of the environment where experiment was carried out and the LiDAR sensor used in it, Quanergy M8. Next, the mathematical description of the three 3D registration methods used in the paper: Iterative Closest Point (ICP), Coherent Point Drift (CPD)

and Normal Distribution Transform (NDT). Then, the algorithm developed to register LiDAR data with the three methods and reconstruct an indoor surface. Finally, experimental results are presented for each registration method and a comparative between them in terms of root mean square error of the Euclidean distance, path obtained and resulting surface.

2 Materials

Both the time sequence of M8 captured point clouds and the Matlab code used to carry out the computational experiments has been published as open data and open source code [1] in the Zenodo repository for reproducibility.

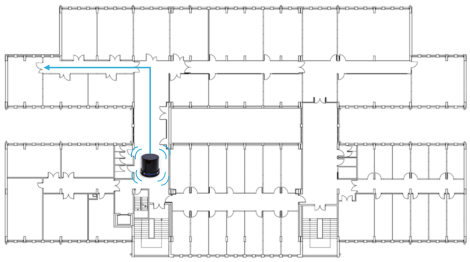

Fig. 1. Nominal path followed during the LiDAR recording.

Location and experiment setting The experiment was carried out in the third floor of the Computer Science School of the UPV/EHU in San Sebastian. Figure 1 shows the nominal path followed by the M8 LiDAR on a manually driven mobile platform. The actual path shows small perturbations around the nominal path. We do not have a precise actual path measurement allowing to quantify the error in the trajectory.

LiDAR M8 Quanergy The Quanergy M8 LiDAR sensor is a multi-laser system with 8 2D line scanners located on a spinning head. The Figure 2 shows the M8 Quanergy LiDAR physical aspect and some of its specifications. This system is based on Time-of-Flight (TOF) technology whose spin rate is between 5 Hz and 20 Hz and its maximum range is 100 m. The Table 1 shows the M8 LiDAR main parameters. Besides, M8 LiDAR comes with 2 desktop applications to manage and visualize point clouds, a SDK to record and show data in real time, and a SDK in framework ROS.

[1] `http://doi.org/10.5281/zenodo.3633727`

Table 1. Quanergy M8 sensor specifications

Parameter	M8 sensor specifications
Detection layers	8
Returns	3
Mininum range	0.5m (80% reflectivity)
Maximum range	>100m (80% reflectivity)
Spin rate	5Hz - 20Hz
Intensity	8-bits
Field of view	Horizontal 306º - Vertical 20º (+3º/-17º)
Data outputs	Angle, Distance, Intensity, Synchronized Time Stamps

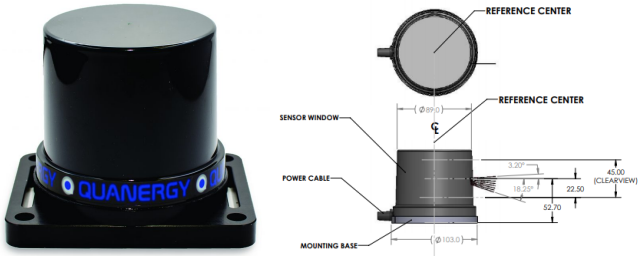

Fig. 2. The M8 Quanergy LiDAR and diagrammatic specs.

3 Point cloud registration methods

Point cloud registration methods are composed of two steps: (a) finding the correspondence between points in one cloud (the moving) to the points in the other cloud (the reference), and (b) the estimation of the motion parameters that achieve optimal match of the moving points to the reference points after correcting for the motion. If the motion is modeled by a rigid body or an affine transformation, then a matrix transformation common to all points is estimated. If the motion is some non linear deformation, then we have to estimate a flow field. In this paper we are restricted to rigid body transformations, which are compositions of a translation and a rotation. The transformation estimation process takes the form of a minimization problem where the energy function is related to the quality of the correspondence achieved. Next we recall the basics of the three point cloud registration methods.

3.1 ICP

The most popular and earlist point cloud registration method is the Iterative Closest Point (ICP) proposed by Besl in 1992 [1]. This technique has been exploited in many domains, giving rise to a host of variations whose relative merits are not so easy to assess [11]. Given a point cloud $P = \{\mathbf{p}_i\}_{i=1}^{Np}$ and a shape described by another point cloud $X = \{\mathbf{x}_i\}_{i=1}^{Nx}$ (The original paper includes the possibility to specify other primitives such as lines or triangles with

well defined distances to a point, but we will not consider them in this paper.) the least squares registration of P is given by $(\mathbf{q}, d) = \mathcal{Q}(P, Y)$, where $Y = \{\mathbf{y}_i\}_{i=1}^{Np}$ is the set of nearest points from X to the points in P, i.e. $\mathbf{p}_i \in P; \mathbf{y}_i = \arg\min_{\mathbf{x} \in X} \|\mathbf{x} - \mathbf{p}_i\|^2$, denoted $Y = \mathcal{C}(P, X)$, and operator $\mathcal{Q}$ is the least squares estimation of the rotation and translation mapping P to Y using quaternion notation, thus $\mathbf{q} = [\mathbf{q}_R \mid \mathbf{q}_T]^t$ is the optimal transformation specified by a rotation quaternion $\mathbf{q}_R$ and a translation $\mathbf{q}_T$, and d is the registration error. The energy function minimized to obtain the optimal registration is $f(\mathbf{q}) = \frac{1}{N_p} \sum_{i=1}^{Np} \|\mathbf{y}_i - \mathbf{R}(\mathbf{q}_R)\mathbf{p}_i - \mathbf{q}_T\|^2$, where $\mathbf{R}(\mathbf{q}_R)$ is the rotation matrix constructed from quaternion $\mathbf{q}_R$. The iteration is initialized by setting $P_0 = P$, $\mathbf{q}_0 = [1, 0, 0, 0, 0, 0, 0]^t$, and $k = 0$. The algorithm iteration is as follows: (1) compute the closest points $Y_k = \mathcal{C}(P_k, X)$, (2) compute the registration $(\mathbf{q}_k, d_k) = \mathcal{Q}(P_0, Y_k)$, (3) apply the registration $P_{k+1} = \mathbf{q}_k(P_0)$, and (4) terminate the iteration if the results are within a tolerance: $d_k - d_{k+1} < \tau$.

3.2 CPD

The Coherent Point Drift (CPD) [10,7] registration method considers the alignment of two point sets as a probability density estimation problem. The first point set $X = \{\mathbf{x}_i\}_{i=1}^{N}$ is considered the data samples generated from the Gaussian mixture model (GMM) whose centroids are given by the second point set $Y = \{\mathbf{y}_i\}_{i=1}^{N}$. Therefore, the CPD registration tries to maximize the likelihood X as a sample of the probability distribution modeled by Y after the application of the transformation $T(Y, \theta)$, where θ are the transformation parameters. The GMM model is formulated as $p(\mathbf{x}) = \omega \frac{1}{N} + (1 - \omega) \sum_{m=1}^{M} \frac{1}{M} p(\mathbf{x} \mid m)$ assuming a uniform distribution for the *a priori* probabilities $P(m) = \frac{1}{M}$, and adding an additional uniform distribution $p(\mathbf{x} \mid M + 1) = \frac{1}{N}$ to account for noise and outliers. All Gaussian conditional distributions are isotropic with the same variance σ^2, i.e. $p(\mathbf{x} \mid m) = \left(2\pi\sigma^2\right)^{-D/2} \exp\left(\frac{\|\mathbf{x} - \mathbf{y}_m\|^2}{2\sigma^2}\right)$. The point correspondence problem is equivalent to selecting the centroid $\mathbf{y}_m$ with maximum *a posteriori* probability $P(m \mid \mathbf{x}_n)$ for a given sample point $\mathbf{x}_n$. The CPD tries to minimize the negative log-likelihood $E\left(\theta, \sigma^2\right) = -\sum_{n=1}^{N} \log \sum_{m=1}^{M} P(m)\, p(\mathbf{x} \mid m)$ by an expectation-maximization (EM) algorithm. The E step corresponds to solving the point correspondence problem using the old parameters, by computing the *a posteriori* probabilities with the old parameters $P^{old}(m \mid \mathbf{x}_n)$. Let $p_{n,m}^{old} = \exp\left(-\frac{1}{2}\left\|\frac{\mathbf{x}_n - T\left(\mathbf{y}_n, \theta^{old}\right)}{\sigma^{old}}\right\|\right)$, then $P^{old}(m \mid \mathbf{x}_n) = p_{n,m}^{old}\left(\sum_{k=1}^{M} p_{k,m}^{old} + c\right)^{-1}$. The M step is the estimation of the new parameters minimizing the complete negative log-likelihood $Q = -\sum_{n=1}^{N} \sum_{m=1}^{M} P^{old}(m \mid \mathbf{x}_n) \log\left(P^{new}(m)\, p^{new}(\mathbf{x} \mid m)\right)$. For rigid transformations, the objective function takes the shape: $Q\left(\mathbf{R}, \mathbf{t}, s, \sigma^2\right) = \frac{1}{2\sigma^2} \sum_{n,m=1}^{N,M} P^{old}(m \mid \mathbf{x}_n) \|\mathbf{x}_n - s\mathbf{R}\mathbf{y}_m - \mathbf{t}\|^2 + \frac{N_p D}{2} \log \sigma^2$ such that $\mathbf{R}^T\mathbf{R} = \mathbf{I}, \det(\mathbf{R}) = 1$. Closed forms for the transformation parameters are given in [10].

3.3 NDT [2]

The key difference of this method is the data is representation. The space around the sensor is discretized into regular overlapped cells. The content of each cell having more than 3 points is modelled by a Gaussian probability distribution of mean $\mathbf{q} = \frac{\mathbf{1}}{\mathbf{n}} \sum_i \mathbf{x}_i$ and covariance matrix $\Sigma = \frac{1}{n-1} \sum_i (\mathbf{x}_i - \mathbf{q}) (\mathbf{x}_i - \mathbf{q})^t$, so that the probability of a LiDAR sample falling in the cell is of the form: $p(\mathbf{x}) \sim \exp\left(-\frac{1}{2}\right) (\mathbf{x} - \mathbf{q}) \Sigma^{-1} (\mathbf{x} - \mathbf{q})$. Given an initial rigid body transformation $T(\mathbf{x}; \mathbf{p}_0)$, where $\mathbf{p}$ is the vector of translation and rotation parameters, a reference point cloud $\{\mathbf{x}_i\}$ modelled by the mixture of the cells Gaussian distributions, and the moving point cloud $\{\mathbf{y}_i\}$, the iterative registration process is as follows: the new laser sample points $\mathbf{y}_i$ are transformed into the reference frame of the first cloud $\mathbf{y}'_i = T(\mathbf{y}_i; \mathbf{p}_{t-1})$, where we find the cell where it falls and use its parameters $(\mathbf{q}, \Sigma)$ to estimate its likelihood $p(\mathbf{y}'_i)$. The score of the transformation is given by $score(\mathbf{p}) = \sum_i p(\mathbf{y}'_i)$. The maximization of the score is carried out by gradient ascent using Newton's method, i.e. $\mathbf{p}_t = \mathbf{p}_{t-1} + \triangle\mathbf{p}$. The parameter update is computed solving the equation $\mathbf{H}\triangle\mathbf{p} = -\mathbf{g}$, where $\mathbf{H}$ and $\mathbf{g}$ are the Hessian and the gradient of the $-score(\mathbf{p}_{t-1})$ function, respectively. Closed forms of $\mathbf{H}$ and $\mathbf{g}$ are derived in [2] for the 2D case. An extension to 3D is described in [8].

4 Registration and SLAM algorithm

Figure 3 presents a flow diagram of the general algorithm that we have applied to obtain the registration of the LiDAR point clouds recorded at each time point $t = \{1, \ldots, T\}$ while the sensor is being displaced manually in the environment according to the approximate path in Figure 1. The final result of the process is a global point cloud $M(T)$ that contains all the recorded 2D points registered relative to the first acquired point cloud $N(0)$, and the estimation of the LiDAR recording positions relative to the initial position. These recording positions are given by the composition of the point cloud registration transformations estimated up to this time instant. The trajectories displayed below all start from the XY plane origin for this reason. The process is as follows: For each acquired point cloud $N(t)$ at time t, firstly we remove the ego-vehicle points denoting $N(1)(t)$ the new point cloud. Secondly we remove the ground plane applying a threshold on the height, obtaining $N(2)(t)$. Thirdly, we downsample the point cloud to decrease the computation time and improve accuracy registration, obtaining $N(3)(t)$. For the initial point cloud at $t = 0$, $N(3)(t)$ becomes the global merged cloud $M(0)$. For subsequent time instants $t > 0$, the fourth step is to estimate the transformation T_t of the aquired data $N(3)(t)$ to the previous global point cloud $M(t-1)$. For this estimation, after applying we use any of the registration algorithms described above to register $T_{t-1}(N(3)(t))$ to $M(t-1)$ obtaining T_t. We then apply this trasformation to the acquired point cloud previous to downsampling $N(4)(t) = T_t(N(2)(t))$, which is used to obtain the new global registed point cloud by merging $M(t) = merge(M(t-1), N(4)(t))$.

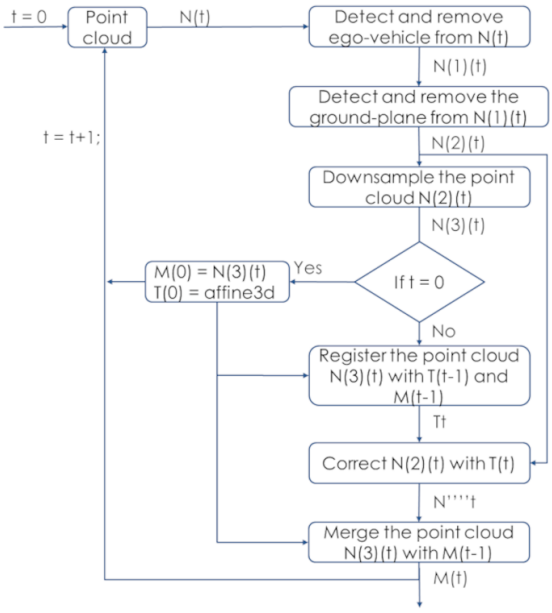

Fig. 3. Flow diagram of the registration algorithm. N(i)(t) is the point cloud at time t after the i-th step of processing. M(t) is the overal point cloud up after merging all the registered point clouds processed up to time t.

5 Results

Figure 4 presents the evolution of the registration error of the SLAM algorithm described in Figure 3 of the point clouds recorded along the path shown in Figure 1 using the three registration methods described in Section 3 alternatively. The plot is logarithmic scale in order to be able to represent the three error plots in the same scale. The NDT algorithm gives the minimal error all along the path. The error of both NDT and CPD registration methods remains bounded, however the error of the ICP method explodes after a point in the trajectory, specifically the turning point at the end of the main hallway in Figure 1. Figure 5(right) shows the overall cloud point obtained at the end of the SLAM porcess, and the estimated trajectory (white points). After some point in the trajectory, the ICP registration loses track and gives random looking results. Figure 5(right) shows the results of the ICP registration up to the turning point, which are comparable with the results of the other algorithms. Figure 6(right) shows the results of the CPD algorithm in terms of the registered and merged overall cloud of points and the trajectory estimation (white points). It can also be appreciated that the SLAM process gets lost after the path turning point, however the registration of point clouds does not become unwieldly. Finally, Figure 7(up) shows the results of the NDT algorithm. The trajectory (white points) is quite accurate to the actual path followed by the sensor. The trajectroy turning point was in fact as smoth as shown in the figure. The overal registered and merged point cloud has a nice fit of the actual hallway walls, as can be appreciated in Figure 7(bottom), including a communication swhich closet signaled in the figure with an arrow, that is not present in the original floor plan.

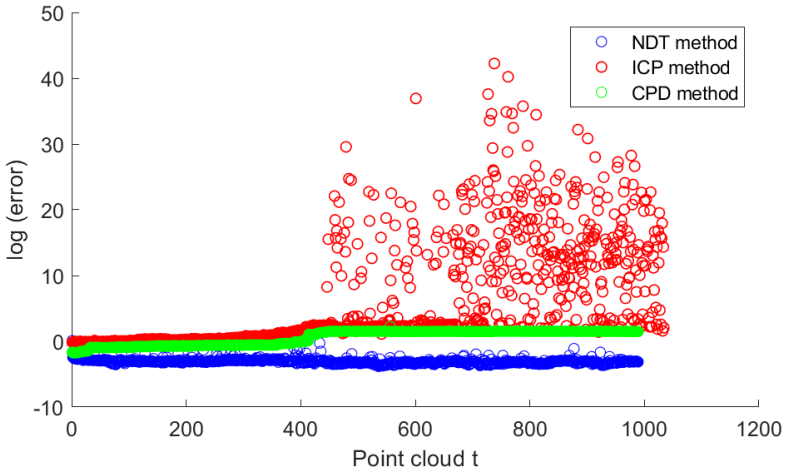

Fig. 4. Evolution of the registration error (log plot) for NDT (blue dots), CPD (green dots), and ICP (red dots).

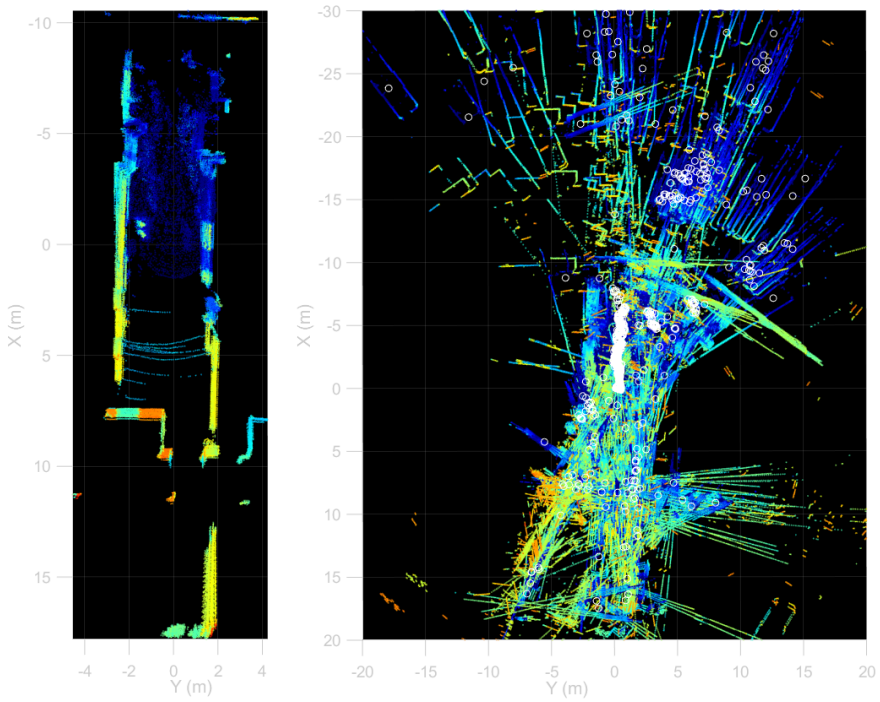

Fig. 5. Estimated trajectory (white points) and registered cloud of points using ICP (right). Registration of the cloud points before reaching the turning point (left).

6 Conclusion

In this paper we report a comparison between three registration methods for 3D point clouds, namely the Iterative Closest Point (ICP), Coherent Point Drift (CPD) and Normal Distributions Transform (NDT). To collect point sets, we have located the M8 Quanergy LiDAR sensor on a manually driven mobile platform through the third floor of the Computer Science School of the UPV/EHU in San Sebastian. The registration algorithm followed in this paper includes preprocessing (detect and remove ego-vehicle and floor, and downsample), registration, transformation and merger point cloud. For each method described in this paper, we have obtained the registration error, the estimation of the path traversed by the sensor, and the reconstructed point cloud. For the ICP and CPD methods, the error is larger than for the NDT method. Besides, after the turning point in the nominal path, ICP and CPD obtained path and resulting point cloud are incorrect. NDT registration obtains coherent experimental results and an accurate trayectory compared with the nomical path followed.

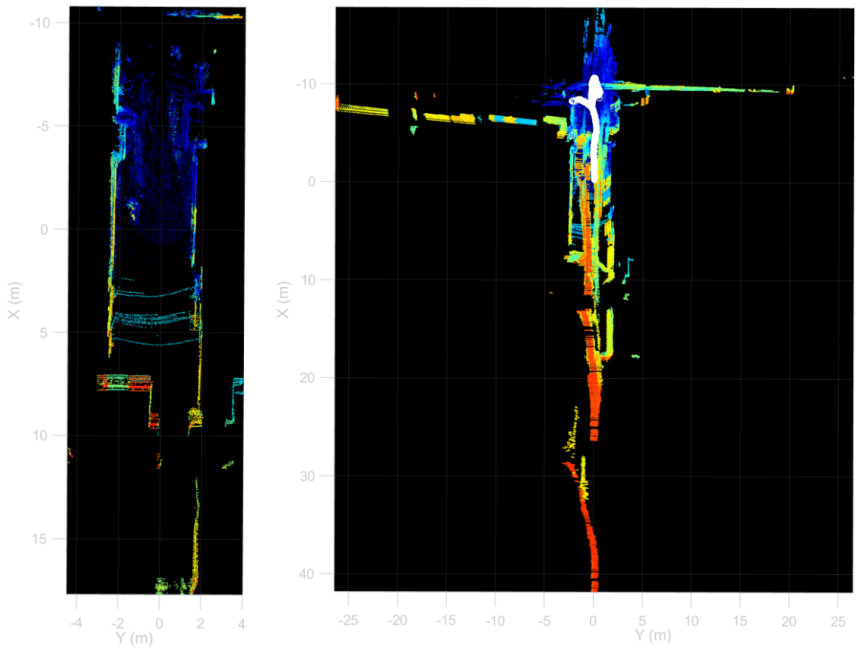

Fig. 6. Estimated trajectory (white points) and registered cloud of points using CPD (right). Registration of the cloud points before reaching the turning point (left).

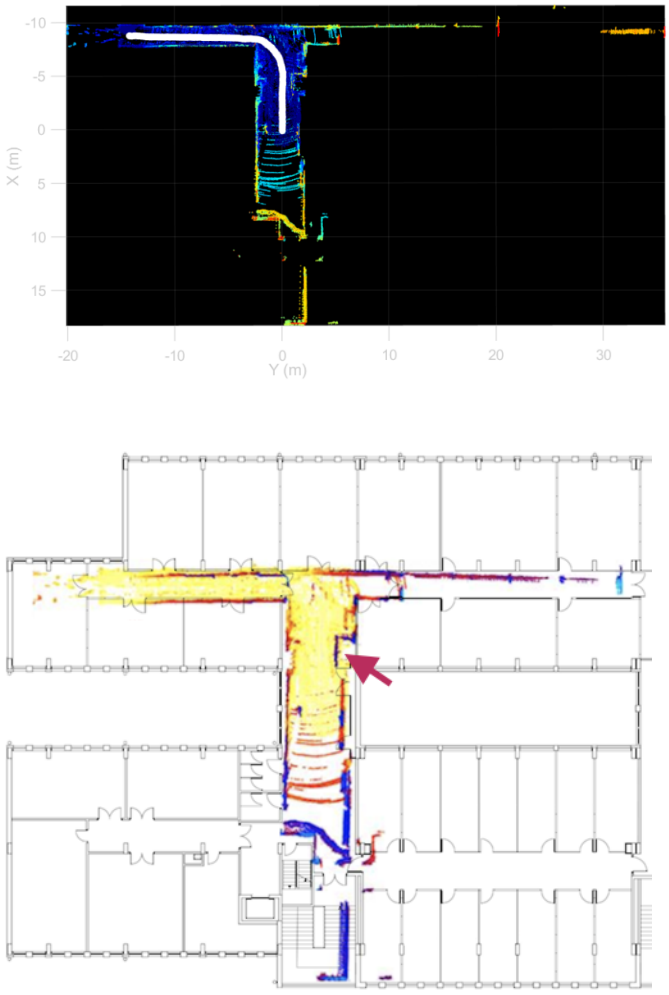

Fig. 7. Estimated trajectory (white points) and registered cloud of points using NDT (Above). Projection of the NDT registered point cloud on the plan of stage 3 of the building.

A future works would be to combine the three methods described in this paper to obtain a better result than obtained separately.

References

1. P. J. Besl and N. D. McKay. A method for registration of 3-d shapes. *IEEE Transactions on Pattern Analysis and Machine Intelligence*, 14(2):239–256, Feb 1992.
2. Peter Biber and Wolfgang Straßer. The normal distributions transform: A new approach to laser scan matching. volume 3, pages 2743 – 2748 vol.3, 11 2003.
3. I. Caminal, J. R. Casas, and S. Royo. Slam-based 3d outdoor reconstructions from lidar data. In *2018 International Conference on 3D Immersion (IC3D)*, pages 1–8, Dec 2018.
4. Y. Deng, Y. Shan, Z. Gong, and L. Chen. Large-scale navigation method for autonomous mobile robot based on fusion of gps and lidar slam. In *2018 Chinese Automation Congress (CAC)*, pages 3145–3148, Nov 2018.
5. J. Levinson and S. Thrun. Robust vehicle localization in urban environments using probabilistic maps. In *2010 IEEE International Conference on Robotics and Automation*, pages 4372–4378, May 2010.
6. Jesse Levinson and Sebastian Thrun. *Unsupervised Calibration for Multi-beam Lasers*, pages 179–193. Springer Berlin Heidelberg, Berlin, Heidelberg, 2014.
7. J. Lu, W. Wang, Z. Fan, S. Bi, and C. Guo. Point cloud registration based on cpd algorithm. In *2018 37th Chinese Control Conference (CCC)*, pages 8235–8240, July 2018.
8. Martin Magnusson, Achim Lilienthal, and Tom Duckett. Scan registration for autonomous mining vehicles using 3d-ndt. *Journal of Field Robotics*, 24:803–827, 10 2007.
9. M. A. Mitteta, H. Nouira, X. Roynard, F. Goulette, and J. E. Deschaud. Experimental Assessment of the Quanergy M8 LIDAR Sensor. *ISPRS - International Archives of the Photogrammetry, Remote Sensing and Spatial Information Sciences*, 41B5:527–531, Jun 2016.
10. A. Myronenko and X. Song. Point set registration: Coherent point drift. *IEEE Transactions on Pattern Analysis and Machine Intelligence*, 32(12):2262–2275, Dec 2010.
11. François Pomerleau, Francis Colas, Roland Siegwart, and Stéphane Magnenat. Comparing icp variants on real-world data sets. *Autonomous Robots*, 04 2013.
12. D. Wu, Y. Meng, K. Zhan, and F. Ma. A lidar slam based on point-line features for underground mining vehicle. In *2018 Chinese Automation Congress (CAC)*, pages 2879–2883, Nov 2018.
13. Z. Xuexi, L. Guokun, F. Genping, X. Dongliang, and L. Shiliu. Slam algorithm analysis of mobile robot based on lidar. In *2019 Chinese Control Conference (CCC)*, pages 4739–4745, July 2019.
14. R. Yagfarov, M. Ivanou, and I. Afanasyev. Map comparison of lidar-based 2d slam algorithms using precise ground truth. In *2018 15th International Conference on Control, Automation, Robotics and Vision (ICARCV)*, pages 1979–1983, Nov 2018.